Dynamics of the Field-Induced Formation of Hexagonal Zipped-Chain Superstructures in Magnetic Colloids

D. Heinrich,[1] A. R. Goñi,[2] A. Smessaert,[3] S. H. L. Klapp,[3] L. M. C. Cerioni,[4] T. M. Osán,[4,5] D. J. Pusiol,[4,5] and C. Thomsen[1]

[1]*Institut für Festkörperphysik, EW 5-4, Technische Universität Berlin, Hardenbergstrasse 36, 10623 Berlin, Germany*
[2]*ICREA and Institut de Ciència de Materials de Barcelona (ICMAB-CSIC), Esfera UAB, 08193 Bellaterra, Spain*
[3]*Institut für Theoretische Physik, EW 7-1, Technische Universität Berlin, Hardenbergstrasse 36, 10623 Berlin, Germany*
[4]*SPINLOCK S.R.L., Avenida Sabattini 5337, Ferreyra, Córdoba X5016LAE, Argentina*
[5]*Facultad de Matemática, Astronomía y Física, Medina Allende s/n, Ciudad Universitaria, Córdoba X5016LAE, Argentina*

(Received 8 June 2010; published 20 May 2011)

Combining nuclear magnetic resonance and molecular dynamics simulations, we unravel the long-time dynamics of a paradigmatic colloid with strong dipole-dipole interactions. In a homogeneous magnetic field, ionic ferrofluids exhibit a stepwise association process from ensembles of monomers over stringlike chains to bundles of hexagonal zipped-chain patches. We demonstrate that attractive van der Waals interactions due to charge-density fluctuations in the magnetic particles play the key role for the *dynamical* stabilization of the hexagonal superstructures against thermal dissociation. Our results give insight into the dynamics of self-organization in systems dominated by dipolar interactions.

DOI: 10.1103/PhysRevLett.106.208301 PACS numbers: 82.70.Dd, 68.08.De, 75.50.Mm, 76.60.−k

Magnetic colloids are a playground for fundamental studies of the interplay between competing interactions of magnetic, electrostatic, and steric nature, which lead to a rich phenomenology as far as the clustering is concerned. A precise knowledge of the conditions under which aggregation of biocompatible ferrofluids occurs in the blood is crucial to avoid complications during medical treatment due to their widespread application as drug carriers and in hyperthermia of tumors [1]. The response to external magnetic fields of systems with strong dipole-dipole (DD) interactions bears self-assembly phenomena such as the formation of field-aligned chains and columns, with a large impact on the magnetorheological properties of the ferrofluid [2,3]. Structuration in the form of chains has been experimentally [4–10] as well as theoretically [11–15] studied. Such self-organization processes are also ubiquitous in a large variety of systems with general dipolar interactions like surfacted semiconductor [16] or core-shell metallodielectric nanoparticles [17] and even fibrous protein aggregates [18]. Here we deal with the *dynamics* of structure formation, which is much less understood. There are few reports of a two-step aggregation process characterized by a faster formation of field-oriented chains and the subsequent but sluggish buildup of pseudocrystalline chain superstructures [9,10,19–21]. These phenomena have been explained, in part, by ground-state calculations like the Halsey-Toor model [22], as modified by Martin *et al.* [11]. A central question concerns the conditions under which neighboring aligned dipolar chains can *attract* each other. Several mechanisms have been proposed, including DD interaction of rigid chains, thermally induced fluctuations, and interactions driven by defects [23]. Depending on the coupling strength and volume fraction, each of these processes dominate the long-time coarsening of the colloidal suspension [4]. Isotropic van der Waals (vdW) interactions, although of particular importance in ionic ferrofluids [24,25] but not exclusively, have been disregarded so far. We demonstrate for the first time that these *attractive* vdW interactions play a crucial role in the robustness of the superstructures against thermal fluctuations.

Experimentally, we make use of the ability of nuclear magnetic resonance (NMR) to distinguish between different magnetic environments of water protons [26] to monitor in real time the clustering of an aqueous ionic ferrofluid (IFF) immersed in a homogeneous field. From the variation with time of the NMR peak amplitude, we infer that the magnetic grains aggregate first to field-aligned chains which subsequently coalesce to form a pseudocrystalline superstructure on time scales of minutes. Molecular dynamics (MD) simulations, including dipolar interactions between the magnetic moments and a Lennard-Jones (LJ) potential to account for vdW interactions due to charge fluctuations in the nanoparticles, yield a very good qualitative description of the association processes revealed by NMR. MD simulations demonstrate that for the coalescence of the previously formed chains into hexagonal bundles, though driven by the lateral magnetic field of the chains, the dynamical stabilization by attractive vdW interactions is a key factor.

The sample consists of an electrostatically stabilized ferrofluid composed of charged magnetite (Fe_3O_4) grains dispersed in water with a particle concentration of 1 vol %. HCl acid is employed to set $p\mathrm{H} = 3$. Particles agglomerate to stable grains of about 100 nm in size on the average. Magnetization measurements indicate superparamagnetic

behavior [27]. About 1 ml of the fluid is loaded into a sealed plastic vial and placed in the bore of a low-resolution SpinLock SLK-100 NMR spectrometer equipped with two permanent supermagnets that generate a uniform field of 225 mT with a homogeneity of 22 ppm and a gradient of 5 μT/cm. Spectra were taken subsequently every 30 s for more than 3000 s.

Figure 1(a) shows a representative NMR spectrum of the IFF sample (solid circles) measured at room temperature at the beginning of a sequence. Frequencies are measured relative to the Larmor frequency of protons in pure water in the NMR field of 225 mT (sharp peak centered at zero frequency). In contrast, the IFF displays a broad and asymmetric peaklike feature which actually consists of two peaks. The main feature with a full width at half maximum (FWHM) of roughly 4 kHz is centered at about 17 kHz, whereas the much weaker and broader peak shows a negligible frequency shift. Both peaks can be attributed to the different environments experienced by protons in the ferrofluid. The frequency shift and line broadening are signatures of strongly inhomogeneous magnetic field and gradient distributions, respectively, produced by the magnetic grains of the ferrofluid and sensed by the protons during their restricted diffusion in the time scale of the NMR experiment (1 ms) [26]. The main peak with the large shift is associated to water protons within layers near and around the magnetic poles of the nanograins (i.e., strong field regions), whereas the secondary feature is assigned to the signal from the water molecules moving freely within the interstitial volume between magnetic particles but far away from them.

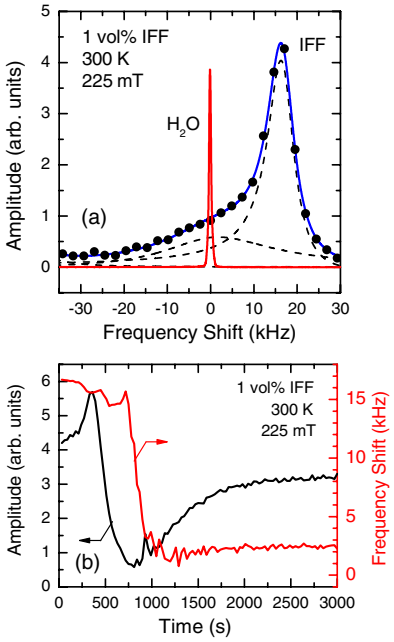

FIG. 1 (color online). (a) Representative NMR spectra of the ionic ferrofluid sample with a concentration of 1 vol % measured at the beginning of a sequence (solid circles). Solid (blue) and dashed (black) curves represent the total NMR line shape function and individual peak terms, respectively. The (red) curve is the NMR spectrum of pure water. (b) Dependence on time of the amplitude and position obtained by fitting the line shape function $S_R(\nu)$ to the main peak of each NMR spectrum of the IFF measured every 30 s.

The real part of the NMR spectral function is $S_R(\nu) = \frac{A\Gamma}{\Delta\nu^2+\Gamma^2}(\Gamma\cos\theta - \Delta\nu\sin\theta)$, as obtained by Fourier transforming the detected signal $S(t)$, where A is the signal amplitude, $\Delta\nu$ is the frequency shift, Γ is the linewidth related to the spin-spin relaxation time and the field-induced inhomogeneous broadening, and θ is the phase shift. The full NMR line shape is obtained by adding an expression like $S_R(\nu)$ for each resonance line. The solid curves through the data points in Fig. 1(a) illustrate the results of nonlinear least-squares fits. The fitted amplitude and position of the most prominent peak in each spectrum are plotted in Fig. 1(b) as a function of time.

The abrupt change in the frequency of the main peak allows for a distinction between two stages in the time evolution of the aggregation state of the IFF. In contrast, the linewidth and phase shift values before and after the transition are similar. The first stage corresponds to the period of gradual aggregation of monomers prior to forming chains. The shift of about 17 kHz is indicative of a strong average magnetic field produced by the oriented magnetic moments of the grains. The peak amplitude exhibits a nonmonotonic behavior with an initial period of 300–400 s, where it shows a slight increase or little change with time. Since in a homogeneous field there is no magnetophoresis, the particles need this time to come closer together solely driven by the long-range dipole-dipole attraction induced by the orientation of the magnetic moments along the field. A steep decrease in amplitude follows, which is triggered by chain formation driven by head-to-tail interactions between particles. The reduction in amplitude is simply explained by the fact that each time two particles form a dimer or one particle adds to a chain, there is a loss of two *high-field* regions corresponding to the magnetic poles which are now in contact. Hence, chain formation leads to a continuous decrease in the number of protons in high-field regions. We point out that the characteristic time of (130 $\pm$ 20) s obtained for the amplitude decrease is in good agreement with the time associated with chain formation in Raman scattering for exactly the same IFF sample [7].

Remarkably, the second stage characterized by a much smaller frequency shift of about 3 kHz proceeds after a time period of about 800 s, when the chains seem to have reached a critical average length. MD simulations show that at this point the sluggish formation of patches of a pseudocrystalline superstructure consisting in bundles of field-oriented, parallel staggered chains sets in. The small frequency shift is indicative of a much lower average magnetic field in the interstitial regions between chains

within bundles. From the amplitude variation we infer that at room temperature and 225 mT this process takes a longer time of (420 ± 50) s. Once the superstructures are formed, they are stable for hours even in the absence of a magnetic field. Immersing the sample in ultrasound bath, though, fully resets structure formation, yielding the original colloidal suspension again.

For a deeper understanding of the association processes we ran MD simulations, employing a simplified model of $N = 1024$ spherical particles with diameter σ and magnetic dipole moment $\boldsymbol{\mu}_i$, completely aligned along the field direction. (Following earlier work on ferrofluids, e.g., Refs. [14,15,28], we neglect any higher multipole corrections [29].) The isotropic part of the two-particle interaction at distance r_{ij} is described by a (truncated and shifted) LJ potential $u_{\mathrm{LJ}}(r_{ij}) = 4\epsilon[(\sigma/r_{ij})^{12} - (\sigma/r_{ij})^{6}]$, where the van der Waals term ($\propto -r_{ij}^{-6}$) models attractive interactions due to charge-density fluctuations in the nanoparticles [24]. The dimensionless LJ parameter is $\epsilon^* = \epsilon/k_BT = 1.0$, k_B and T being the Boltzmann constant and the temperature, respectively. For the anisotropic contribution mimicking the magnetic DD interaction, we employ the *screened* potential $(\boldsymbol{\mu}_i\nabla_i)(\boldsymbol{\mu}_j\nabla_j) \times [\exp(-\kappa r_{ij})/r_{ij}]$ (with $\kappa\sigma = 1$). Using this effectively short-ranged potential saves much computational time without altering the physics qualitatively. We also restrict ourselves to two-dimensional (2D) systems with a packing fraction of $\eta = (\pi/4)\rho\sigma^2 = 0.015$, very close to the experiment. The strength of the dipolar magnetic coupling is determined by the parameter $\lambda = \mu^2/k_BT\sigma^3$, where $\mu = |\boldsymbol{\mu}_i|$ is a function of the saturation magnetization and size of the particles. We just set $\lambda = 7$, where pronounced association is known to occur from previous simulation studies of 2D dipolar systems [12]. Calculations are performed at constant T, by using a time step of $\Delta t = 0.0025$. Typical MD runs consisted of about 10^8 time steps in total.

Figure 2 shows snapshots illustrating the particle configuration on the way towards equilibrium. Simulations started from translationally ordered, quadratic states, but the diluted system loses the initial information quickly after a few thousand MD steps. The typical configuration then involves only monomers. During subsequent times, the association into long dipolar strings oriented along the field occurs [see Fig. 2(a)]. The development of large peaks, separated by well-defined minima, in the quasi-instantaneous correlation function $g_{\parallel}(r_{ij})$ in the field direction [30] is the signature of chain formation. Figure 2(a) also includes data for the perpendicular correlation function $g_{\perp}(r_{ij})$ [30], which is essentially zero at the time considered. This changes at later times, where snapshots reveal lateral association of the strings into *bundles* with hexagonal ordering of the chains [see Fig. 2(b)]. Note that the main peak of $g_{\perp}(r_{ij})$ is shifted towards somewhat larger distances relative to that of $g_{\parallel}(r_{ij})$, consistent with the fact that the chains are staggered; hence, the particles in

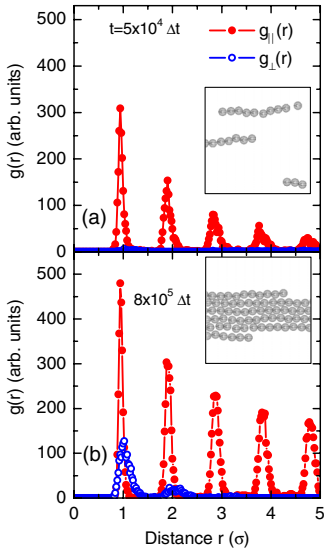

FIG. 2 (color online). MD simulation snapshots (insets) at various times on the way towards equilibration. Full (red) and open (blue) symbols represent the quasi-instantaneous correlation functions parallel and perpendicular to the field, respectively.

two neighboring chains are shifted by half a diameter relative to one another. This hexagonal-like arrangement is known to minimize the energy in systems of aligned dipolar chains [4,28] (the hexagonal bond-order parameter [30] at long times is $\Psi_6 \approx 0.8$).

We now consider the heights of the main peak in the correlation functions of $g_{\parallel(\perp)}$ as *order parameters* for the association process. In Fig. 3, we plot these quantities as functions of time. For times $t \lesssim 50\,000\Delta t$ we observe a strong increase of $g_{\parallel}^{\max}$, while $g_{\perp}^{\max} \approx 0$. This is the regime of string formation corresponding to the first stage of the

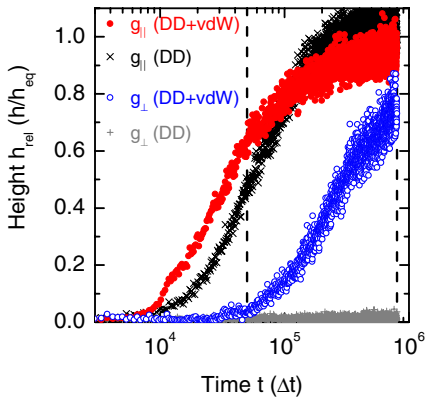

FIG. 3 (color online). Time dependence of the first maximum of the parallel (red) and perpendicular (blue) correlation functions (normalized to their equilibrium values). Vertical lines indicate the times corresponding to Figs. 2(a) and 2(b). Results for the system without vdW interactions (black and gray symbols) are also included.

NMR experiments (high-frequency shift). The coalescence of the chains into bundles starts when $g_{\perp}^{\max} \neq 0$. This occurs when the average chain length is ≈ 4. Thus, our data reveal a clear two-step process for the field-induced structure formation in excellent semiquantitative agreement with the experimental findings.

Lateral aggregation starts only when the strings are already present in full agreement with ground-state calculations [28]. Even at $T = 0$ attractive interactions in *lateral* directions occur only for chains of sufficient lengths and at high enough densities. At finite temperatures, thermal fluctuations tend to hinder this effect. The striking result is that, by cutting off the vdW interaction ($\propto -r_{ij}^{-6}$), we do not find evidence for the hexagonal ordering, as seen in Fig. 3. This remains true also for smaller values of the shielding parameter κ. In the supplemental material (videos) [31], the mechanism by which the additional attractive vdW interaction leads to the dynamical stabilization of the superstructures can be visualized. Its main effect is to slow down chain motion such that the interaction time between colliding chains increases as much as necessary for the short-range lateral magnetic coupling to be effective, promoting superstructure formation even at room temperature.

In summary, we found out that the aggregation dynamics of ionic magnetic colloids in a homogeneous field exhibits subsequent stages of evolution characterized by an increasingly hierarchical ordering. Strikingly, the existence of strong dipole-dipole interactions alone is not sufficient to warrant the long-time *crystallization* of zipped-chain superstructures at the densities of interest. As demonstrated by the 2D molecular dynamics simulations, a long-range van der Waals attraction due to charge fluctuations in the nanoparticles acts as a catalyst for superstructure formation, working against thermal dissociation. This conclusion is also supported by NMR measurements on *weakly ionic* citrate-based ferrofluids, which exhibit superstructure formation only if placed in an inhomogeneous magnetic field for more than 120 s [32]. Our results enlighten the clustering dynamics of magnetic fluids and open up the combination of NMR with MD simulations as a powerful tool to study more complex systems like biofunctionalized nanoparticle colloids, amyloid assembly, or nanocomposites such as ferronematics and ferrogels.

Special thanks are due to N. Buske from MagneticFluids for the ferrofluid samples. This work was supported by DAAD, Germany, and SECYT, Argentina, through the PROALAR2007 program. A. S. was supported by the German DFG within the IRTG 1524 project. L. M. C. C., T. M. O., and D. J. P. thank CONICET, Argentina, for financial support.

[1] R. Jurgons *et al.*, J. Phys. Condens. Matter **18**, S2893 (2006).
[2] S. H. Lee and C. M. Lindell, Small **5**, 1957 (2009).
[3] C.-H. Chang *et al.*, Nanotechnology **20**, 495301 (2009).
[4] E. M. Furst and A. P. Gast, Phys. Rev. E **62**, 6916 (2000).
[5] A. Wiedenmann *et al.*, Phys. Rev. E **68**, 031203 (2003).
[6] M. Klokkenburg *et al.*, Phys. Rev. Lett. **97**, 185702 (2006).
[7] D. Heinrich *et al.*, J. Chem. Phys. **126**, 124701 (2007).
[8] W.-X. Fang *et al.*, Europhys. Lett. **77**, 68 004 (2007).
[9] F. Martínez-Pedrero *et al.*, Phys. Rev. E **78**, 011403 (2008).
[10] J. M. Laskar, J. Philip, and B. Raj, Phys. Rev. E **80**, 041401 (2009).
[11] J. E. Martin *et al.*, J. Chem. Phys. **108**, 3765 (1998).
[12] J. J. Weis, Mol. Phys. **103**, 7 (2005).
[13] A.-P. Hynninen and M. Dijkstra, Phys. Rev. Lett. **94**, 138303 (2005).
[14] P. Ilg, Eur. Phys. J. E **26**, 169 (2008).
[15] J. Jordanovic and S. H. L. Klapp, Phys. Rev. Lett. **101**, 038302 (2008).
[16] Z. Zhang *et al.*, Nano Lett. **7**, 1670 (2007).
[17] S. Gangwal *et al.*, Soft Matter **6**, 1413 (2010).
[18] J. Dudowicz *et al.*, J. Chem. Phys. **130**, 224906 (2009).
[19] A. Wiedenmann *et al.*, Phys. Rev. Lett. **97**, 057202 (2006).
[20] C. Rablau *et al.*, Phys. Rev. E **78**, 051502 (2008).
[21] F. Donado, U. Sandoval, and J. L. Carrillo, Phys. Rev. E **79**, 011406 (2009).
[22] T. C. Halsey and W. Toor, Phys. Rev. Lett. **65**, 2820 (1990).
[23] J. E. Martin, K. M. Hill, and C. P. Tigges, Phys. Rev. E **59**, 5676 (1999).
[24] F. Cousin, E. Dubois, and V. Cabuil, Phys. Rev. E **68**, 021405 (2003).
[25] S. M. Garcia *et al.*, Nano Lett. **5**, 169 (2005).
[26] C. E. González *et al.*, J. Chem. Phys. **109**, 4670 (1998).
[27] See supplemental material at http://link.aps.org/supplemental/10.1103/PhysRevLett.106.208301 for further sample characterization.
[28] R. Tao and J. M. Sun, Phys. Rev. Lett. **67**, 398 (1991).
[29] H. Ma *et al.*, Adv. Phys. **52**, 343 (2003).
[30] R. A. Trasca and S. H. L. Klapp, Comput. Phys. Commun. **179**, 66 (2008).
[31] See supplemental material at http://link.aps.org/supplemental/10.1103/PhysRevLett.106.208301 for video material on MD simulations.
[32] D. Heinrich, A. R. Goñi, L. M. C. Cerioni, T. M. Osán, D. J. Pusiol, and C. Thomsen (to be published).